Ultra-compact Silicon 90° Optical Hybrid by Adjoint-based Inverse Design Method

Shanglin Yang*
School of Optoelectronic Engineering
Xidian University
Xi'an, China
*yangshanglin@xidian.edu.cn

Hao Jia
School of Physical Science and Technology
Lanzhou University
Lanzhou, China
jiahao@lzu.edu.cn

Yue Yu
School of Optoelectronic Engineering
Xidian University
Xi'an, China
yyu@xidian.edu.cn

Han Zheng
School of Optoelectronic Engineering
Xidian University
Xi'an, China
hzheng_0323@stu.xidian.edu.cn

***Abstract*—We demonstrate an ultra-compact 2×4 90° optical hybrid with adjoint-based inverse design method. The device footprint is 6.4 μm × 4.4 μm. For S and R-light input, the insertion losses are less than 0.78 dB.**

Keywords—Inverse design; silicon photonics; 90° optical hybrid

I. INTRODUCTION

In recent years, coherence optical communications are promising to be commercially applied in optical systems. 90° optical hybrid, as a key component in DSP-based optical demodulation in coherence modulation format such as the QPSK, has recently attracted considerable research attention [1].

However, the traditional 90° optical hybrid is based on the principle of multimode interference, and its size is typically on the order of server hundred micrometers [2].

The essence of on-chip optical device design is to search a geometric structure in the solution space to make the evaluation function meet the requirements under the constraints of Maxwell's equations and the material and size constraints. In recent years, as a new type of photonics design method, inverse design has achieved many devices with ultra-compact and high-efficiency characteristics [3, 4]. Through inverse design optimization, the designer can search the geometric structure in the solution space more deeply.

This paper uses the inverse design method to design an ultra-compact silicon 2×4 90° optical hybrid. The method is based on density material parameterization [5] and the adjoint method [6]. The device's footprint is 6.4 μm × 4.4 μm, and the insertion loss 0.78 dB for the S-light input and 0.76 dB for the R-light input.

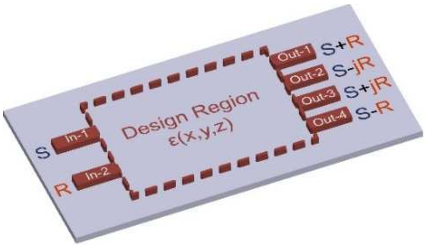

Fig.1. Function schematic diagram of the 2×4 90° optical hybrid.

II. DEVICE DESIGN

We show the function of the 2×4 90° optical hybrid in Fig. 1. The device divides input S-light into four outputs equally, and the four output lights have the same phase. For R-light input, the device also divides the light intensity equally, but the phases of the output lights corresponding to the Out-1 ~ Out-4 are 0°, –90°, 90°, and 180°, respectively. The phase 0° is consistent with the output phase of S-light. We choose the platform a commercial silicon-on-insulator (SOI) wafer with 220 nm top silicon layer, 3 μm buried oxide layer and silicon dioxide cladding. The working wavelength is set to 1550 nm. The design task is to search for the distribution of the relative permittivity ε in the design area in Fig. 1, so that the device can realize the functions mentioned above. We can use a mathematical optimization problem to describe the design problem,

$$\begin{aligned} &\max FOM(E,H,\varepsilon) \\ &s.t.\ \ g(E,H,\varepsilon)=0 \end{aligned} \tag{1}$$

where, FOM is the device's figure of merit, and g(E,H,ε) is Maxwell's electromagnetic equations.

We choose the energy coupling efficiency of the input port and the output port as the FOM to evaluate the structures in this task. For the S-light input, the input mode is $\left|\begin{matrix}\mathrm{TE_0}\\0°\end{matrix}\right\rangle_S$, and the target output mode is $\left|\left|\begin{matrix}\mathrm{TE_0}\\0°\end{matrix}\right\rangle_{out-1}+\left|\begin{matrix}\mathrm{TE_0}\\0°\end{matrix}\right\rangle_{out-2}+\left|\begin{matrix}\mathrm{TE_0}\\0°\end{matrix}\right\rangle_{out-3}+\left|\begin{matrix}\mathrm{TE_0}\\0°\end{matrix}\right\rangle_{out-4}\right\rangle_S$. The corresponding mode coupling efficiency is FOM_1. And for the R-light input, the input mode $\left|\begin{matrix}\mathrm{TE_0}\\0°\end{matrix}\right\rangle_R$, and the corresponding target output mode is $\left|\left|\begin{matrix}\mathrm{TE_0}\\0°\end{matrix}\right\rangle_{out-1}+\left|\begin{matrix}\mathrm{TE_0}\\-90°\end{matrix}\right\rangle_{out-2}+\left|\begin{matrix}\mathrm{TE_0}\\90°\end{matrix}\right\rangle_{out-3}+\left|\begin{matrix}\mathrm{TE_0}\\180°\end{matrix}\right\rangle_{out-4}\right\rangle_R$. We define the energy coupling efficiency of the input and output modes as FOM_2. Where TE0 represents the mode order of the corresponding waveguide, and the angle is the relative phase value of different output ports. Then we let the total $FOM_{Total} = FOM_1 \times FOM_2$.

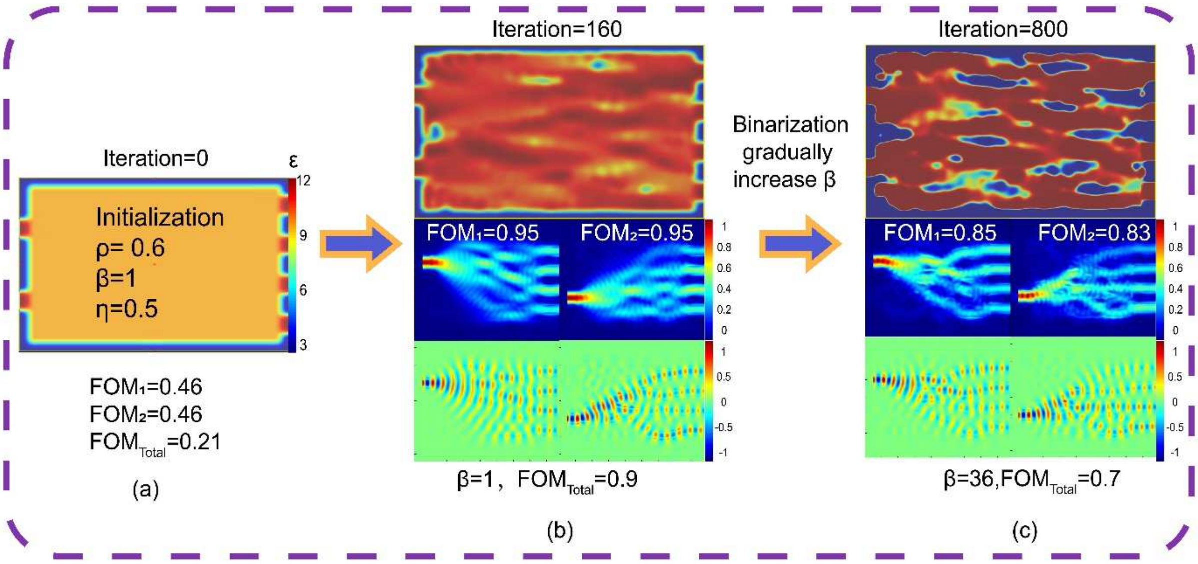

Fig.2. Device optimization process. (a) The initial structure and optimization parameters. (b) The optimization result obtained by retaining β = 1. (c) The device structure and FOM value when β = 36.

In the design strategy, to express the permittivity ε(x,y,z), we use density-based material parameterization. This method first introduces a normalized design variable ρ, and the final ε value is obtained as follows,

$$\tilde{\rho}_i = \frac{\sum_{j\in \mathrm{N}_i} \omega(\mathbf{x}_j)\rho_j}{\sum_{j\in \mathrm{N}_i} \omega(\mathbf{x}_j)}, \quad \omega(\mathbf{x}_j) = R - \left|\mathbf{x}_i - \mathbf{x}_j\right|, \tag{2}$$

$$\bar{\rho}_i = \frac{\tanh(\beta\cdot\eta) + \tanh(\beta\cdot(\tilde{\rho}_i - \eta))}{\tanh(\beta\cdot\eta) + \tanh(\beta\cdot(1-\eta))}, \tag{3}$$

$$\varepsilon_i = \varepsilon_{\min} + (\varepsilon_{\max} - \varepsilon_{\min})\bar{\rho}_i \,. \tag{4}$$

In Eq. (2), $\omega(\mathbf{x}_j)$ is the two-dimensional linear hat-shape filter [5]. The β in Eq. (3) is the projection parameter that controls the intensity of the projection. In the optimization process, we gradually increasing the value of β to make $\bar{\rho}_i$ gradually tend to 0 or 1.

To determine how to modify the value of the design parameter ρ_i, according to adjoint method ,we use forward simulation and adjoint simulation to calculate the gradient $\mathrm{d}FOM/\mathrm{d}\varepsilon(x,y,z)$. Then, use the chain rule of derivative to get the gradient of FOM respect to the design variable $\mathrm{d}FOM/\mathrm{d}\rho_i$. Based on the gradient, we update the design variable ρ_i with the method of moving asymptotes (MMA) [7].

We use MATLAB code to implement the optimization strategy and use Lumerical FDTD solutions to simulate the electromagnetic field. MATLAB processes the field data and performs the iteration.

III. Design Process and Result

A. Optimization Process

We show the device optimization process in Fig. 2. First, as shown in Fig. 2(a), we set the initial design variable $\rho = 0.6$. We keep the parameter $\beta = 1$ unchanged in the first stage. In this case, ε_i in the design region can take any value in [ε_{SiO2}, ε_{Si}], which is conducive to the algorithm to search for higher performance structures. After 160 iterations, the device structure is shown in Fig. (b). The corresponding FOM value is $FOM_{Total} = 0.9$, $FOM_1 = 0.95$, $FOM_2 = 0.95$. Fig. (b) shows the simulated electric field distribution of the input S and R-light field at the In-1 port and In-2 port. It is worth noticing that the device's performance, at this time, is the optimal value in the entire optimization process. However, this structure cannot be implemented to on-chip manufacturing due to its permittivity having many intermediate values [ε_{SiO2},ε_{Si}]. Then we perform the binarization stage. In this stage, we still use the MMA algorithm to iterate the ρ_i but gradually increase the value of β. In Fig. (c), we show an intermediate result in the binarization process. The iteration is 800 and β is 36. As shown in figure, the area with intermediate value is reduced, and most of the area has been binarized. Meanwhile, the FOM value also decreased, and FOM_{Total} is about 0.7. We show the simulated electric field distribution in Fig. 2(c).

B. Result

Finally, we terminate the algorithm terminates at 1600 iterations, and the β value is 128. We cut off the ρ value and set the ρi greater than 0.5 to 1 and the ρ less than 0.5 to 0. The final layout of the device is shown in Fig. 3. The device footprint is 6.4 μm × 4.4 μm. All input and output waveguides are 0.5 μm width. The gap between the two input waveguides is 1.5 μm, and the output waveguides gaps are 0.6 μm. The structure of the device is complex, irregular and non-intuitive. These complex structures affect light waves at the micro-nano level, which reduces the device's size to achieve ultra-compactness.

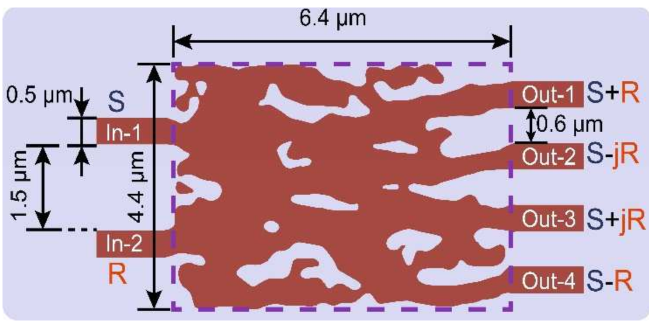

Fig.3. Schematic diagram of optimized device layout.

Fig. 4 shows the simulation results of the device. The FDTD simulation wavelength is 1550 nm, and the simulation mesh is 20nm. Fig. 4(a) is a schematic diagram of the field

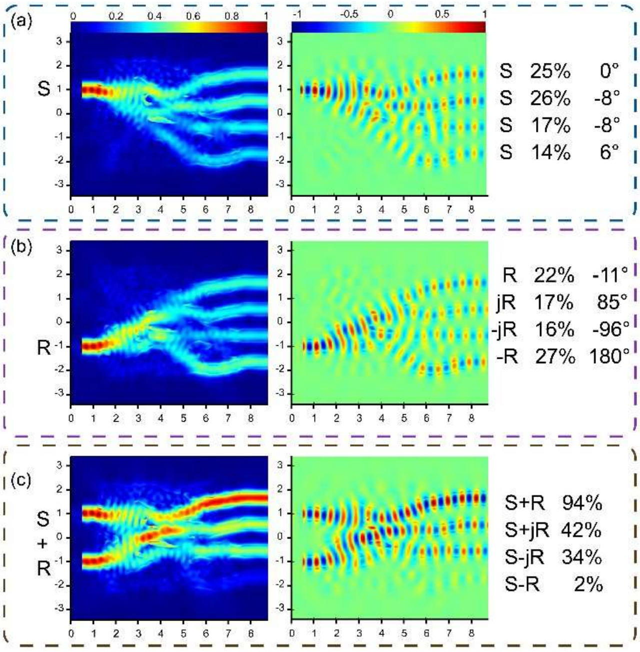

Fig.4. Simulation results of the device. (A) The simulated electric field magnitude and E_y component corresponding to S-light input. (B) The magnitude and E_y component corresponding to R-light input. (C) The simulated electric field intensity and E_y component corresponding to S and R-light input.

intensity and E_y component distribution of the S-light input from the In-1 port. The device divides the S-light into four channels. We use the phase of Out-1 port as the reference phase, which is defined as 0°. The intensity and phase corresponding to the four output ports are (25%, 0°), (26%, –8°), (17%, –8°) and (14%, 6°). Fig. 4(b) shows the corresponding electric field intensity and E_y component when R light is input from In-2 port. Similarly, we still use the phase of the S-Out1 light as the reference phase. At this time, the four outputs corresponding to the R light are (22%, –11°), (17%, 85°), (16%, –96). °) and (27%, 180°). Fig. 4(c) shows the device's electric field intensity and E_y response when S and R light are input together with the same phase. In this case, the total input light intensity is 2, and the output light intensity of the Si four channels is 94%, 42%, 34%, and 2%, respectively.

IV. Conclusion

In conclusion, using the inverse design method, we designed an ultra-compact silicon 2×4 90° optical hybrid. The device footprint is 6.4 µm × 4.4 µm. The simulation results show that the insertion loss of the device for the S-light input is 0.78 dB, and the phase deviations of the four ports do not exceed 8°. For the R-light input, the insertion loss of the device is less than 0.76 dB, and the phase deviations are less than 11°.

References

[1] L. G. Kazovsky, L. Curtis, W. C. Young, and N. K. Cheung, "All-fiber 90° optical hybrid for coherent communications," Applied Optics, vol. 26, Feb. 1987, pp. 437-439.

[2] R. Halir, G. Roelkens, A. Ortega-Moñux, and J. G. Wangüemert-Pérez, "High-performance 90° hybrid based on a silicon-on-insulator multimode interference coupler," Optics Letters, vol. 36, Jan. 2011, pp. 178-180.

[3] B. Shen, P. Wang, R. Polson, and R. Menon, "An integrated-nanophotonics polarization beamsplitter with 2.4 × 2.4 µm2 footprint," Nat. Photonics, vol. 9, May. 2015, pp. 378-382,.

[4] A. Y. Piggott, J. Lu, K. G. Lagoudakis, J. Petykiewicz, T. M. Babinec, and J. Vuckovic, "Inverse design and demonstration of a compact and broadband on-chip wavelength demultiplexer," Nat. Photonics, vol. 9, Jun. 2015, pp. 374-377.

[5] M. D. Zhou, B. S. Lazarov, F. W. Wang, and O. Sigmund, "Minimum length scale in topology optimization by geometric constraints," Comput. Meth. Appl. Mech. Eng., vol. 293, Aug. 2015, pp. 266-282,.

[6] C. M. Lalau-Keraly, S. Bhargava, O. D. Miller, and E. Yablonovitch, "Adjoint shape optimization applied to electromagnetic design," Opt. Express, vol. 21, Sep. 2013, pp. 21693-21701,.

[7] K. Svanberg, "A Class of Globally Convergent Optimization Methods Based on Conservative Convex Separable Approximations," SIAM J. Optim. vol. 12, Jan. 2002, pp. 555-573,.